(23) Roovers, J. *Macromolecules* **1984**, *17*, 1196.
(24) Marrucci, G. In *Advances in Transport Processes*; Mujumdar, A. S., Mashelkar, R. A., Eds.; Wiley: New York, 1984; Vol. 4.
(25) Klein, J. *Macromolecules* **1986**, *19*, 105.
(26) Doi, M.; Edwards, S. F. *The Theory of Polymer Dynamics*; Oxford: 1986.
(27) Viovy, J. L., et al. *J. Polym. Sci., Part B* **1983**, *21*, 2427.
(28) Doi, M. *J. Polym. Sci., Part B* **1983**, *21*, 667.
(29) Tassin, J. F. Thesis, University of Paris VI, 1986.
(30) Wales, J. L. S. *The Application of Flow Birefringence to Rheological Studies of Polymer Melts*; Delft: 1976.
(31) Marrucci, G., submitted to *J. Non Newtonian Fluid Mech.*
(32) Mackley, M.; Mead, D., unpublished results.
(33) Ball, R. C., private communication.
(34) Cogswell, F. N. *Polymer Melt Rheology: A Guide for Industrial Practice*; Goodwin: London, 1981.

# Effect of Elongational Flow on Polymer Adsorption

**G. J. Besio,† R. K. Prud'homme,* and J. B. Benziger**

*Princeton University, Department of Chemical Engineering, Princeton, New Jersey 08544.*
*Received May 28, 1987; Revised Manuscript Received October 6, 1987*

ABSTRACT: The adsorption and desorption of polystyrene (PS) from cyclohexane at 34.8 °C (θ temperature) on a chrome mirror has been studied by using ellipsometry. Static adsorption measurements give adsorbed layer thickness and adsorbed amounts in agreement with previous investigators. The effect of elongational flow on polymer adsorption and desorption was studied by directing a jet of polymer solution or solvent perpendicular to the mirror surface, to produce an elongational velocity field at the stagnation point on the surface. For a $10^7$ $M_w$ PS adsorbed under strong elongational flow conditions, the adsorbed layer was an order of magnitude thinner than a layer adsorbed under quiescent conditions and the polymer concentration in the layer adsorbed under elongational flow was 3.4 times higher. The effect of elongational flow of solvent on the desorption of a polymer layer formed under quiescent conditions was studied. No desorption was observed at the stagnation point. The impinging solvent jet produced a distinctive pattern on the chrome mirror in the desorption experiments. A "bull's-eye" pattern was visible on the dried mirror, showing a center circle of adsorbed polymer, a clear annular ring where shear forces desorbed the polymer, and a region of adsorbed polymer out beyond the desorbed ring.

## Introduction

Polymer adsorption from flowing solutions is important in applications such as enhanced oil recovery, pigment dispersion, and flow-enhanced flocculation. The effect of flow conditions on polymer adsorption has received little attention, because it is difficult to impose a controlled flow field while simultaneously monitoring adsorption. Notable exceptions are recent studies by Robertson,[1,2] using attenuated total reflection spectroscopy (ATR), and Fuller,[3,4] using ellipsometry to study adsorption in shear flow.

Shear flows produce small changes in molecular conformation in dilute solution, whereas elongational flows can produce large conformational changes. In elongational flow fields, when the elongational strain rate, $\dot{\epsilon}$, exceeds the relaxation time of the polymer molecule, $\tau$, the molecule undergoes a coil–stretch transition and becomes highly elongated.[5-7] The coil–stretch transition in an elongational flow field has been directly observed in crossed-flow birefringence by Keller who inferred from the difficulty in cleaning his apparatus that polystyrene sulfonate adsorbed irreversibly when adsorbed from a solution in a stretched state.[5] However, there was no direct evidence as to the nature of the polymer layer adsorbed under stretched-state conditions. In this paper we report an ellipsometric study of polystyrene adsorption in an elongational flow, produced by an impinging jet.

## Polystyrene Adsorption

**A. Summary of Static Experiments.** A comprehensive study of the adsorption of polystyrene was carried out by Takahashi and co-workers[8] who studied the adsorption of polystyrene of molecular weights ranging from 10 000 to 13 000 000 onto chrome from cyclohexane at the θ temperature (34.8 °C). From these studies, the following trends were observed: (1) the thickness of the adsorbed layer scales with molecular weight to the $^1/_2$ power at low molecular weight, (2) above a molecular weight of 300 000 the surface concentration reaches a plateau at about ~5.0 mg/m$^2$, and (3) the surface concentration is independent of solution concentration above a solution concentration of approximately 1000 ppm.

By monitoring the thickness and refractive index of the adsorbed layer at sequential time steps. Takahashi was able to determine approximate adsorption kinetics. The thickness of the adsorbed layer was found to reach a value close to 80% of its equilibrium value within minutes, however, it took approximately 2–3 h to reach a steady-state value. The surface concentration, $A$, was calculated by $A = (n_f - n_m)\delta/(dn/dc)$, where $\delta$ is the thickness of the adsorbed layer, $n_f$ is the refractive index of the adsorbed layer, $n_m$ is the refractive index of the surrounding medium, and $dn/dc$ is the refractive index increment.

**B. Influence of Shear Flow.** Fuller and Lee[3,4] studied two different effects of flow on adsorption with ellipsometry. In the first experiment, a preadsorbed polymer layer was subjected to a shear flow of pure solvent resulting in "flow-enhanced desorption". In a second experiment, adsorption was carried out from a flowing solution resulting in "flow-inhibited adsorption".

Fuller and Lee found that substantial desorption was induced by shear flow. The desorption was initially rapid, becoming negligible after 30 to 40 min. The amount desorbed increased with increasing shear rate for all polymers and also increased with increasing molecular weight. Interestingly, the thickness of the adsorbed layer was not greatly influenced by the flow-induced desorption, except at the highest molecular weight, indicating that little conformational change was induced in the adsorbed layer by flow.

† Current address: General Electric CRD, P. O. Box 8, Building K-1, 4B33, Schenectady, NY 12301.

0024-9297/88/2221-1070$01.50/0 

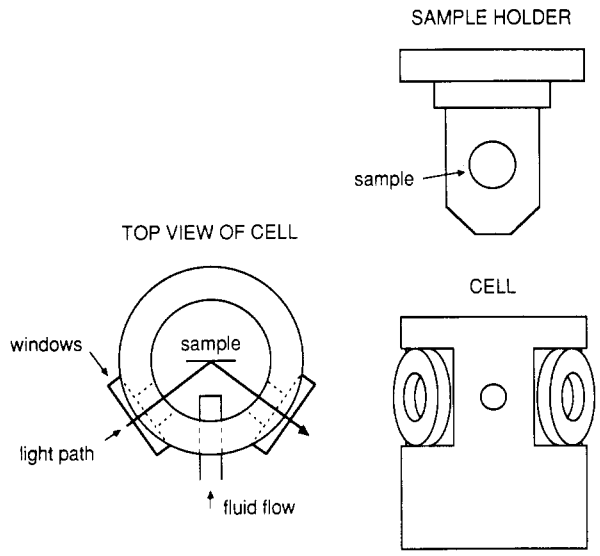


**Figure 1.** Schematic illustration of cell design showing location of flow tube for impinging jet.

In flow-inhibited adsorption, polymer solution was flowed over the adsorbing substrate while the thickness and refractive index of the layer formed were measured ellipsometrically. In general, the approach to a steady-state coverage was slowed and the final surface concentration decreased with increasing shear rate; however, the thickness of the adsorbed layer was unaffected. During flow-inhibited adsorption, the shear rates necessary to inhibit adsorption were less than those necessary to desorb a preadsorbed layer.

## Materials and Apparatus

The two polymers used were monodisperse polystyrene standards obtained from Polymer Laboratories (Amherst, MA). The first was a linear polystyrene of molecular weight $1.8 \times 10^6$ with a polydispersity index of 1.05. The second was a linear polystyrene of molecular weight $20 \times 10^6$ with a polydispersity index of 1.20. The polymer solutions were prepared at concentrations of 1000 ppm for the $1.8 \times 10^6$ $M_w$ sample and 700 ppm for the $20 \times 10^6$ $M_w$ sample. The cyclohexane was spectral grade (Fisher Chemical) and was used as received. Chrome mirrors were prepared by electroplating a thick layer of chrome onto a 19-mm-diameter brass disk which had been polished to a mirror finish. Prior to an adsorption experiment, the disk was cleaned by polishing with alumina paste of grain size <0.05 μm, followed by immersion in a 50/50 mixture of nitric and sulfuric acids for 10 min. The surface was then rinsed with a stream of distilled water, dried, and then stored under pure solvent until use. A nickel-plated brass cell with glass windows was constructed and is shown schematically in Figure 1. The cell temperature was controlled to ±0.1 °C by means of Minco (Minco, In) film heaters affixed to the outside of the cell. The cell was jacketed with insulating foam rubber to provide better temperature control.

Ellipsometry experiments were carried out on a rotating compensator ellipsometer (RCE) constructed in our laboratory. The device is described in detail elsewhere.[10,11] In ellipsometry, the change in polarization of light upon reflection is used to probe the thickness and refractive index of adsorbed layers. In an RCE, the waveform of the detected intensity is used to determine the ellipsometric parameters Δ and Ψ.

The adsorbing substrate was immersed in the polymer solution at 34.8 ± 0.1 °C during the entire course of the experiment. The solutions were kept at the Θ temperature prior to use. Since the polymer would precipitate out of solution at room temperature, care had to be taken in their handling.

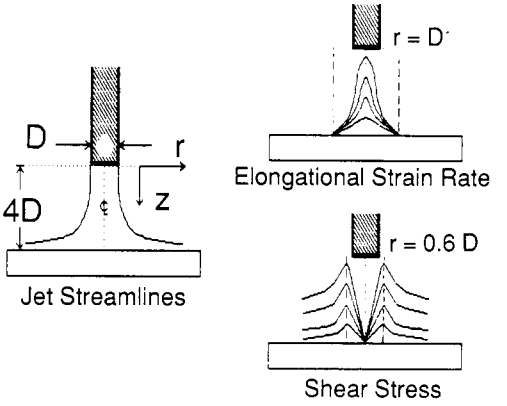


**Figure 2.** Detailed figure of the jet geometry. The jet of diameter $D$ is located $4D$ from the adsorbing surface. The elongational strain rate $\dot{\epsilon}$ is shown for several values of the flow rate. The maximum $\dot{\epsilon}$ value occurs along the center line, and the elongation rate drops to near zero by $r \approx D$. The shear stress is shown which is zero along the center line and has its maximum value at $r = 0.6D$. Calculations are from ref 12 and 13.

The elongational flow was generated by directing the fluid normal to the absorbing surfaces by using an "impinging jet". The solution was pumped with a peristaltic pump (Cole-Parmer, Chicago, IL) through Viton tubing (tubing size no. 15). The tubing was preconditioned to remove any solubles by pumping pure solvent for a period of 12 h. The length of tubing was kept to a minimum to reduce heat losses from the solution to negligible levels.

The impinging jet configuration is illustrated in Figure 2. The inner diameter of the jet nozzle was 3.2 mm. The distance from the tip of the nozzle to the sample surface was 4 jet diameters. It has been shown, by numerical modeling, that this confined laminar impinging jet is stable.[12,13]

## Experiments

**A. Characterization of the Jet.** Preliminary experiments were carried out to measure the effect of jet flow on the ellipsometry measurement by using pure solvent. Although the signal-to-noise ratio of the data increased, it was found that Δ and Ψ measurements with and without flow were the same. The measured standard deviation in both Δ and Ψ, for a single waveform, increased by an order of magnitude; for quiescent conditions, the standard deviation was on the order of ±0.05°, and under flow, it was on the order of ±0.5°. The effects of the flow-induced noise could be reduced by signal averaging, at the expense of temporal resolution.

The flow field of an impinging jet has been characterized mathematically.[11,12] The radial velocity in the stagnation region is given by

$$u_r = ar\bar{v}_j/D \tag{1}$$

where $a$ is a constant which is a weak function of the Reynolds number, $r$ is the radial position, $\bar{v}_j$ is the average velocity of the jet, and $D$ is the jet diameter (which in our apparatus was $^1/_{16}$-in. i.d. and $^3/_{16}$-in. o.d.). The elongational strain rate, $\dot{\epsilon}$, is given by the derivative of the radial velocity at the center line of the jet.

$$\dot{\epsilon} = du_r/dr = a\bar{v}_j/D \tag{2}$$

The elongational strain occurs in the fluid just above the surface upon which the jet is impinging. Below the elon-

**Table I**
**Characterization of the Impinging Jet**

| pump speed setting | flow rate,[a] $Q$, cm$^3$/s | mean jet velocity,[a] $\bar{v}_j\|_{z=0}$, cm/s | elongational strain rate,[b] $\dot{\epsilon}\|_{r=0}$, s$^{-1}$ | jet Reynolds no.,[b] $Re\|_{r=0}$ | max wall shear rate,[b] $\dot{\gamma}_w\|_{r=0.6D}$, s$^{-1}$ |
|---|---|---|---|---|---|
| 2 | 2.5 | 31 | 360 | 750 | 5700 |
| 3 | 3.9 | 49 | 570 | 1190 | 11600 |
| 4 | 5.3 | 66 | 760 | 1600 | 18000 |
| 5 | 6.7 | 84 | 970 | 2000 | 25900 |

[a] Defining equations: $A = \pi D^2/4$, where $D = 0.32$ cm, $\bar{v}_j|_{z=0} = Q/A$. [b] Defining equations: $\dot{\epsilon} = a\bar{v}_j/D$, where $a = 3.70$; $Re = \bar{v}_j D\rho/\mu$ for cyclohexane at 35 °C; $\rho = 0.765$ g/cm$^3$ and $\mu = 1.011 \times 10^{-2}$ g/cm s); $\tau_w|_{r=0.6D} = u_{max}/\delta$, where $\delta$ is the viscous boundary layer thickness; $u_{max} = a\bar{v}_j r/D$, $r = 0.6D$; $\delta = 1.95D/(aRe)^{1/2}$.

**Table II**
**Critical Deborah Number[a]**

| pump speed setting | elongational strain rate, $\dot{\epsilon}$, s$^{-1}$ | $De_{PS\text{-}1.8}$ | $De_{PS\text{-}20}$ |
|---|---|---|---|
| 2 | 360 | 0.02 | 0.8 |
| 3 | 570 | 0.03 | 1.3 |
| 4 | 760 | 0.04 | 1.7 |
| 5 | 970 | 0.05 | 2.1 |

[a] Defining equations: $De_{crit} = \tau_H\dot{\epsilon} \geq 0.5$, where $\tau_H$ = Hookean relaxation time = $[\eta]\eta_s M_w/RT$; $\tau_{H,(PS\text{-}1.8)} \simeq 0.05$ ms; $\tau_{H,(PS\text{-}20)} \simeq 2.2$ ms.

gation zone is a very thin boundary layer dominated by shear flow—but the thickness of this boundary layer is very thin. The expression for the boundary layer thickness is given in the legend of Table I.

Approximate shear and elongational strain profiles for the jet are illustrated in Figure 2. The flow conditions for the experiments are given in Table I.

The Reynolds number for the jet is given by

$$Re_{jet} = \bar{v}_j D\rho/\mu \quad (3)$$

From the tabulated Reynolds number values for the jet, it can be seen that the jet is laminar for all of the experimental conditions investigated. The elongational strain $\dot{\epsilon}$, spans approximately 1 order of magnitude in the experiments reported here. Polymer deformation (coil–stretch transition) occurs when the critical Deborah number exceeds 0.5:[5,6,14]

$$De_{crit} = \tau_H\dot{\epsilon} \geq 0.5 \quad (4)$$

where where $\tau_H$ is the Hookean relaxation time for the molecule which may be estimated by

$$\tau_H = [\eta]\eta_s M_w/RT \quad (5)$$

where $[\eta]$ is the intrinsic viscosity of the solution, $\eta_s$, is the solvent viscosity, $M_w$ is the polymer molecular weight, and $R$ and $T$ have their usual meaning. The relaxation time for the polymers used and the Deborah numbers for the experiments are shown in Table II. For the lower molecular weight polymer, no strong stretching is expected, whereas the high molecular weight polymer should be in the stretched state at all flow rates.

**B. Adsorption in Elongational Flow.** The thickness and refractive index of the adsorbed layer were measured ellipsometrically while the polymer solution was directed at the chrome mirror. The adsorption was monitored for 2 h. Representative plots of $\Delta$ and $\Psi$, as a function of time, are presented in Figure 3 for the quiescent adsorption and adsorption under three different flow rates for the $20 \times 10^6$ $M_w$ polymer. The lowest pump speed was not used in these experiments since it was found that the pump pulsations created an excessively noisy signal. Figures 4 and 5 are the measured film thicknesses and refractive indices as a function of maximum elongational strain rate. Both

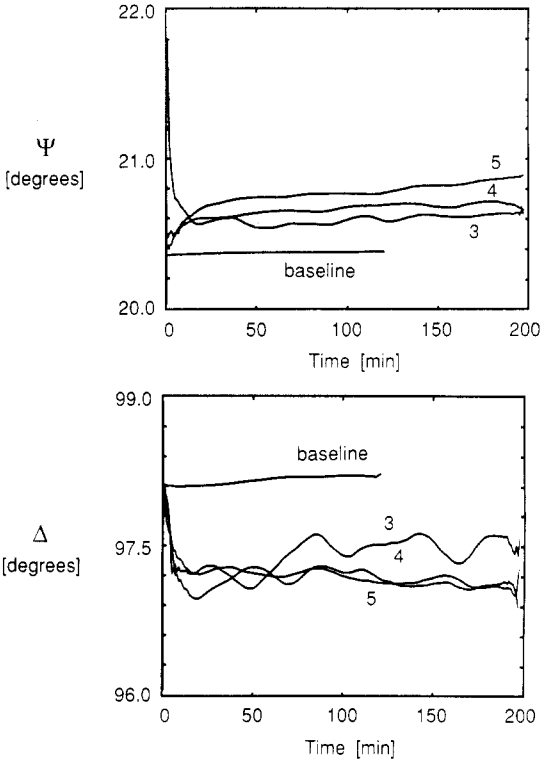


**Figure 3.** Plot of ellipsometric parameter $\Psi$ versus time (top) and $\Delta$ versus time (bottom) during adsorption experiments. The flow rates of the jet are shown on the figures and correspond to pump settings in Table II. Data are for the $20 \times 10^6$ $M_w$ polystyrene sample.

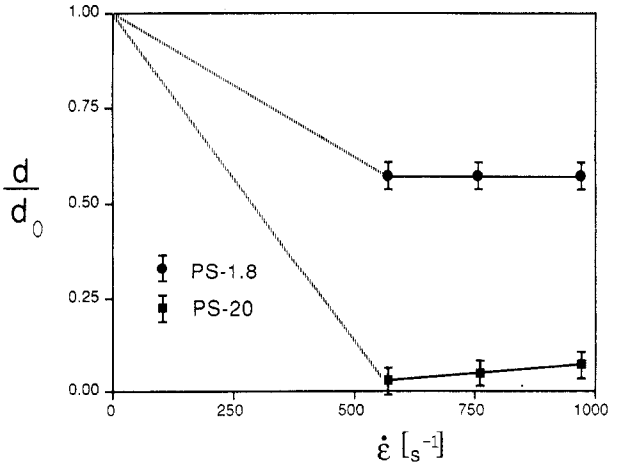


**Figure 4.** Adsorption under elongational flow. Normalized thickness of the adsorbed layer, $d/d_0$ versus maximum elongational strain rate, $\dot{\epsilon}$, for the $1.8 \times 10^6$ $M_w$ (PS-1.8) and $20 \times 10^6$ $M_w$ (PS-20) samples.

samples showed decreases in layer thickness and increases in refractive index under elongational flow. The thickness

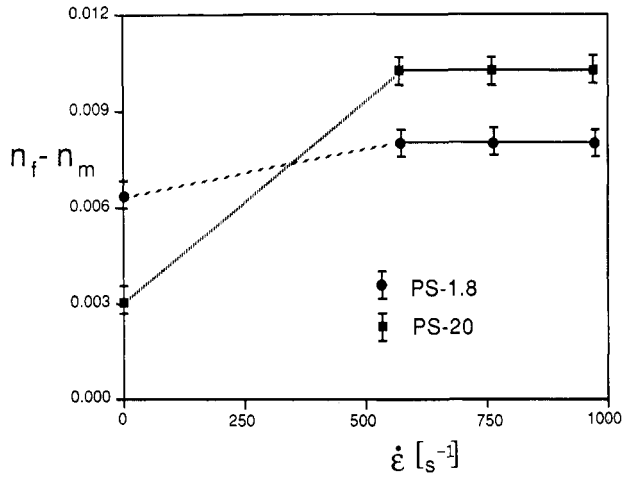


**Figure 5.** Adsorption under elongational flow. Refractive index difference between the film and solution ($n_f - n_m$) versus maximum elongational strain rate, $\dot{\epsilon}$, for the $1.8 \times 10^6$ $M_w$ (PS-1.8) and $20 \times 10^6$ $M_w$ (PS-20) samples.

**Table III**
**Static Adsorption at the Θ Temperature[a]**

| sample | $M_w$ | $M_w/M_n$ | $A_0$, mg/m$^2$ | $d_0$, Å |
|---|---|---|---|---|
| | | This Study | | |
| PS-1.8 | $1.8 \times 10^5$ | 1.05 | 2.3 ± 0.3 | 700 ± 80 |
| PS-20 | $20 \times 10^5$ | <1.20 | 4.7 ± 0.4 | 2900 ± 200 |
| | | Fuller and Lee[3,4] | | |
| PS-4 | $3.8 \times 10^6$ | 1.05 | 4.15 | 1700 |
| PS-8 | $8.4 \times 10^6$ | 1.17 | 4.66 | 2250 |
| PS-20 | $20.0 \times 10^6$ | <1.20 | 4.60 | 3100 |
| | | Takahashi et al.[8] | | |
| FF-33 | $2.4 \times 10^6$ | 1.07 | 4.49 | 1060 |
| FF-35 | $7.6 \times 10^6$ | 1.05 | 4.85 | 1710 |
| FF-37 | $13.4 \times 10^6$ | 1.05 | 4.63 | 2055 |

[a] Defining equations: $A_0 = (n_f - n_m)d_0/(dn/dc)$, where $n_f$ and $d_0$ are the measured film refractive index and thickness and $n_m$ = 1.415 (cyclohexane, 34.8 °C, λ = 6328 Å).

for the lower molecular weight sample, (PS-1.8) under flow was 400 ± 100 Å, with a surface concentration of 1.9 ± 0.5 mg/m$^2$. The thickness of the adsorbed layer was reduced by 40% relative to quiescent adsorption, and the refractive index of the adsorbed film (proportional to the concentration in the adsorbed film) increased by 26%.

For the higher molecular weight sample (PS-20) in elongational flow, the adsorbed layer thickness decreased by 95% (i.e., from 2900 to 150 Å) and the refractive indices of the films and surface concentration of adsorbed polymers increased by 330% (i.e., from 0.003 to 0.010). The adsorbed layer is thinner but much denser than layers adsorbed under quiescent conditions. For all the pump rates used, the critical Deborah number was exceeded for PS-20, suggesting that the molecules are highly stretched and adsorb in a tightly bound compressed configuration on the surface.

**C. Desorption in Elongational Flow.** Desorption enhanced by an impinging jet was examined by adsorbing a layer from a quiescent solution, draining the solution from the cell, and then introducing preheated solvent into the cell. A base-line measurement was made after refilling the cell, flow was then initiated, and the adsorbed layer was followed for approximately 1 h. After an hour a second base line was obtained with the flow off.

The results for adsorption from a quiescent fluid were similar to those of previous studies, although the surface concentration reported here is slightly less. The data for

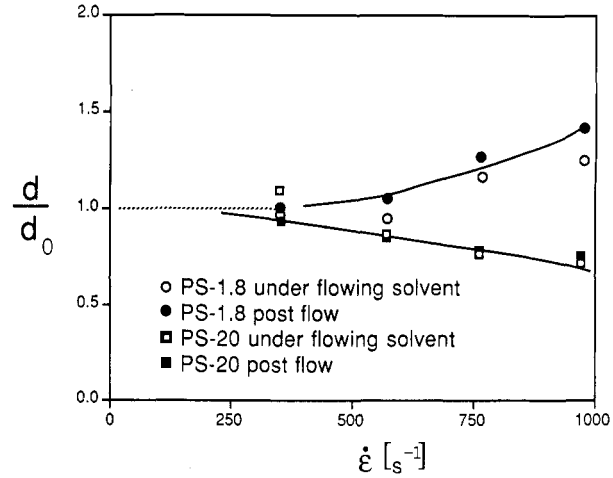


**Figure 6.** Desorption under elongational flow. Normalized thickness of the adsorbed layer, $d/d_0$, versus maximum elongational strain rate, $\dot{\epsilon}$. Measurements are taken during solvent flow (open symbols) and immediately after the cessation of flow (filled symbols) for PS-1.8 (circles) and PS-20 (squares).

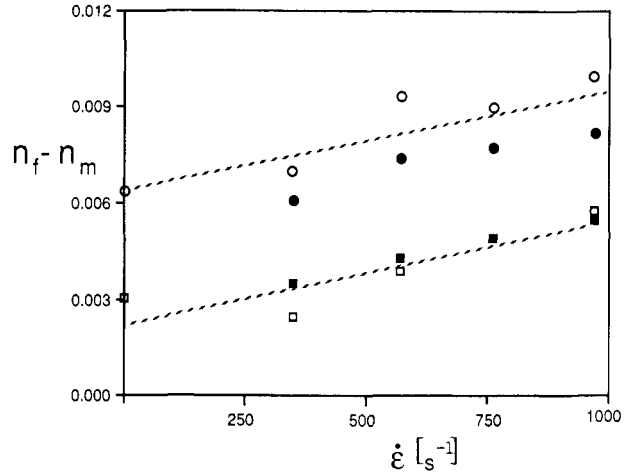


**Figure 7.** Desorption under elongational flow. Refractive index difference between the film and solution ($n_f - n_m$) versus maximum elongational strain rate, $\dot{\epsilon}$. Symbols are defined as in Figure 6.

layer thickness and the surface concentration from a quiescent fluid are presented in Table III. Figures 6 and 7 show the adsorbed layer thickness and film refractive index as functions of solvent elongational strain rate. For the higher molecular weight sample, PS-20, the layer thickness decreased with increasing strain rate and the refractive index of the layer increased. This indicated that the jet compressed the adsorbed layer. However, the surface concentration of polymer in the adsorbed layer was not conserved, but increased with time. Additional polymer appears to be deposited over the hour-long flow experiment. This polymer may be coming from small amounts of residual polymer solution left in the cell after draining the initial polymer solution. Also, polymer may be present that was desorbed by flow and redeposited at the stagnation point where the ellipsometric measurement was made. When the chrome mirror was removed from the sample cell at the end of a desorption experiment a "bull's-eye" pattern emerged on the mirror as it dried. The pattern is illustrated in Figure 8. The pattern consists of (i) a central circle corresponding to the adsorbed layer under the impinging jet, (ii) a shiney ring which appeared to have no adsorbed polymer, and (iii) a hazy ring. The ring without adsorbed polymer would correspond to the region where the shear rates were high enough to desorb the polymer. The shear rates decrease in the radial di-

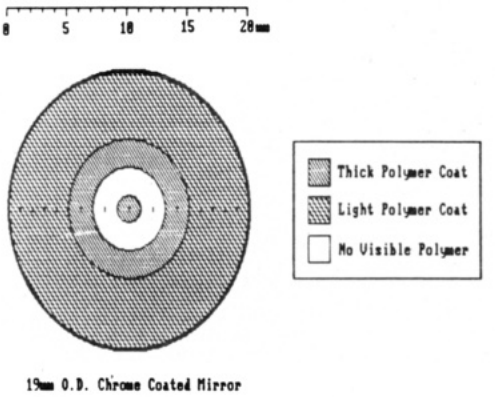


**Figure 8.** Schematic illustration of the "bull's-eye" adsorption pattern caused by impinging solvent jet on a preadsorbed layer.

rection and so the hazy ring represents the transition from the region of complete desorption to the region of equilibrium adsorption where the shear flow does not affect the preadsorbed layers.

For the lower molecular weight sample, the thickness of the adsorbed layer increased with increasing flow rate. The reason for this is unclear, but we believe it is due to the buildup of recirculating polymer at the stagnation point of the flow. When the flow is turned off the thickness of the adsorbed layer decreases (Figure 6), indicating that some of these trapped chains are only weakly adsorbed, so that they diffuse away after flow is stopped. In the desorption experiments similar values of the ellipsometric parameters were measured while the solvent was flowing and after it had been stopped. This indicates that solution birefringence effects due to any dissolved polymer were insignificant.

## Summary

The results of the adsorption studies show that the adsorption of polymers is dramatically affected by elongational flow. Polymers adsorbed from elongational flow fields, which are strong enough to produce stretched-state conformations, result in highly compressed and dense adsorbed layers. This suggests that the polymer chains are attached to the substrate at many more sites than if they had adsorbed from a quiescent solution. This different adsorbed conformation might provide stronger polymer/substrate adhesion—this appears to be an area for further study. Polymers adsorbed quiescently and then subjected to an elongational flow field of solvent appeared to redistribute on the surface. After exposure to an impinging jet a "bull's-eye" pattern could be observed on the dried mirror surface showing the region of adsorption under elongational flow, a region of shear-induced desorption, and the outer region of polymers adsorbed under equilibrium conditions.

**Acknowledgment.** We thank American Cyanamid Co. (fellowship for G.B.) and the National Science Foundation (Presidential Young Investigator Award for R.K.P.) for generous financial support. Construction of the ellipsometer was made possible by a grant from Du Pont.

**Registry No.** Polystyrene, 9003-53-6.

## References and Notes

(1) Lok, B. K.; Cheng, Y.; Robertson, C. R. *J. Colloid Interface Sci.* **1983**, *91*, 87.
(2) Lok, B. K.; Cheng, Y.; Robertson, C. R. *J. Colloid Interface Sci.* **1983**, *91*, 87.
(3) Lee, J. J.; Fuller, G. G. *Macromolecules* **1984**, *17*, 375.
(4) Lee, J. J.; Fuller, G. G. *J. Colloid Interface Sci.* **1985**, *103* (2), 569.
(5) Miles, M. J.; Tanaka, K.; Keller, A. *Polymer* **1983**, *24*, 1081.
(6) Scrivener, O.; Berner, C.; Cressely, R.; Hocquart, R.; Sellin, R.; Vlancos, N. S. *Polymer* **1975**, *5*, 475.
(7) Cressely, R.; Hocquart, R. *Proceedings of the VIII International Congress on Rheology*; Astarita, G., Ed.; Naples, Italy, 1980; p 377.
(8) Takahashi, A.; Kawaguvhi, M.; Hirota, H.; Kato, T. *Macromolecules* **1980**, *13*, 884.
(9) Killmann, E.; Eisenlauer, J.; Korn, M. *J. Polym. Sci., Polym. Symp.* **1977**, *No. 61*, 413.
(10) Besio, G. J. Ph.D. Thesis, Princeton University, 1986.
(11) Besio, G. J.; Prud'homme, R. K.; Benziger, J. B. submitted for publication to *Langmuir*.
(12) Law, H.-S.; Masliyah, J. H. *Ind. Eng. Chem. Fund.* **1984**, *23*, 446.
(13) Deshpande, M. D.; Vaishav, R. N. *J. Fluid Mech.* **1982**, *114*, 213.
(14) Inerthal, W.; Hass, R. *Proc., Euromech., Delft, Holland* **1981**, *143*, 157.